

Primary pulmonary malignant fibrous histiocytoma: case report and literature review

Xiongfei Li^{1*}, Renwang Liu^{1*}, Tao Shi^{2*}, Shangwen Dong³, Fan Ren¹, Fan Yang¹, Dian Ren¹, Haiyang Fan¹, Sen Wei¹, Gang Chen¹, Jun Chen^{1,4}, Song Xu^{1,4}

¹Department of Lung Cancer Surgery, ²Department of Pathology, ³Department of Cardiothoracic Surgery, ⁴Tianjin Key Laboratory of Lung Cancer Metastasis and Tumor Microenvironment, Lung Cancer Institute, Tianjin Medical University General Hospital, Tianjin 300052, China

*These authors contributed equally to this work.

Correspondence to: Jun Chen, MD, PhD. Department of Lung Cancer Surgery, Lung Cancer Institute, Tianjin Medical University General Hospital, No. 154 Anshan Road, Heping District, Tianjin 300052, China. Email: huntercj2004@yahoo.com; Song Xu, MD, PhD. Department of Lung Cancer Surgery, Lung Cancer Institute, Tianjin Medical University General Hospital, No. 154 Anshan Road, Heping District, Tianjin 300052, China. Email: xusong198@hotmail.com.

Abstract: Malignant fibrous histiocytoma (MFH) is an aggressive soft tissue sarcoma known to occur in various organs. Primary MFH arising in the lung is quite rare. Herein we report a case of a 61-year-old male with primary pulmonary MFH and explore the underlying molecular mechanisms by next-generation sequencing (NGS). Five gene mutations in TSC2, ARID1B, CDK8, KDM5C and CASP8 were detected, and the mTOR inhibitor might be an effective treatment for this patient. In addition, we reviewed the scientific literature of approximately 23 primary pulmonary MFH case reports since 1990 and summarized the clinical features and prognosis of this rare pulmonary malignant tumor.

Keywords: Malignant fibrous histiocytoma (MFH); sarcoma; surgery; sequencing

Submitted Mar 03, 2017. Accepted for publication Jul 03, 2017.

doi: 10.21037/jtd.2017.07.59

View this article at: <http://dx.doi.org/10.21037/jtd.2017.07.59>

Introduction

Malignant fibrous histiocytoma (MFH) is an aggressive soft tissue sarcoma originating from mesenchymal tissues (1). It is one of the most common soft tissue sarcomas in adults and can also affect juveniles (1). Although MFH can develop in various organs, it most commonly occurs in the extremities and the retroperitoneal space of the abdominal cavity (2). However, primary MFH arising in the lung is rare (3). Since the first case reported in 1979, there have been approximately 36 reported cases of primary pulmonary MFH. Primary pulmonary MFH is highly malignant, and there are no optimal or consensus treatment strategies (4). In order to find a better treatment and improve the survival rate, we performed next-generation DNA sequencing (NGS) of MFH tissue from a 61-year-old male with primary pulmonary MFH. In addition, we summarized the clinical features and prognosis of this rare pulmonary malignant

tumor based on the published literature (4-23).

Case presentation

A 61-year-old male with a 40-year heavy smoking history was admitted with chief complaints of an intermittent cough and blood expectoration for 10 days. Computed tomography (CT) scans revealed an 8 cm × 7 cm × 5 cm mass in the right upper lobe with large lymph nodes present in the hilum and mediastinum (*Figure 1*). Subsequent physical examination revealed reduced respiratory sounds over the right upper lung field. Laboratory tests revealed a high expression of neuron-specific enolase (NSE) (19 µg/L, range: 0–16.3 µg/L), aspartate aminotransferase (AST 47 U/L, range: 15–46 U/L), creatine kinase (CK 180 U/L, range: 30–170 U/L), creatine kinase-isoenzyme (CK-MB 27 U/L, range: 0–24 U/L) and urea (8.0 mmol/L, range 2.5–7.1 mmol/L). Radiological tests revealed no

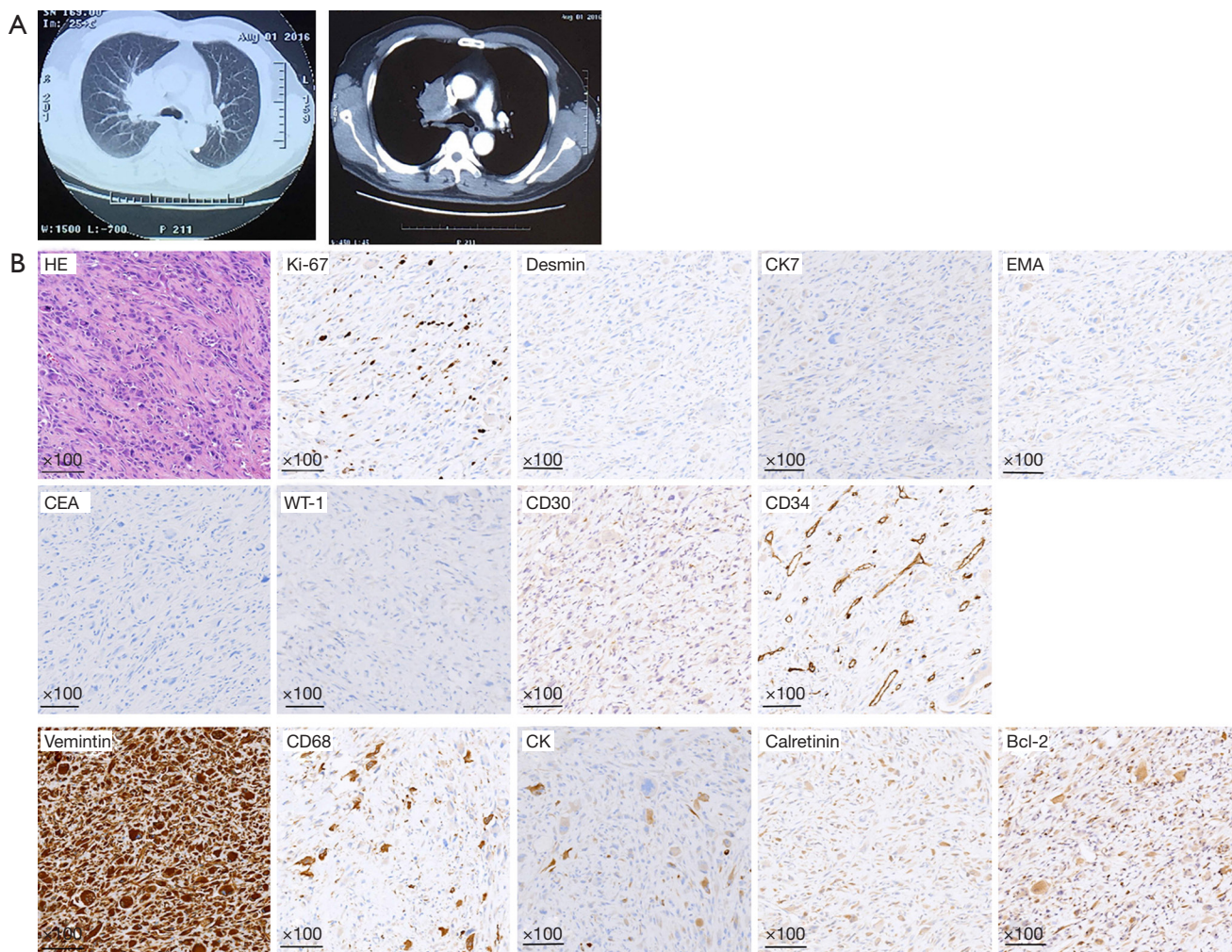


Figure 1 CT images, H&E and immunohistochemical staining results. (A) Chest CT shows an 8 cm × 7 cm × 5 cm mass in the right upper lobe with large lymph nodes present in the hilum and mediastinum; (B) H&E staining shows irregularly shaped infiltrating cells with abnormal nuclei and prominent nucleoli. IHC staining shows diffuse positivity for vimentin and partial positivity for CD68, CK, CD68, calretinin and Bcl-2 with a Ki67 index of approximately 10% and negativity for desmin, CK7, EMA, CEA, WT-1, CD34 and CD30.

significant abnormalities in the abdomen, brain or bone. A bronchoscopy was performed of the interlobar crest of the right upper lobe and rapid on-site evaluation (ROSE) revealed necrosis and morphologically heterogeneous cells. Histopathological examination further showed evidence of squamous metaplasia with moderate atypical hyperplasia, including lymphocyte and neutrophil infiltration.

Following this initial examination, the patient underwent a right upper lobectomy and systemic lymphadenectomy with bronchial sleeve resection and subsequent reconstruction of the pulmonary artery and superior vena cava. Immunohistochemical staining of tumor tissue demonstrated positivity for vimentin,

CK (Cytokeratin), CD68, calretinin and Bcl-2 with a Ki-67 proliferative index of approximately 10%. In contrast, tumors were deemed negative for desmin, CK7, epithelial membrane antigen (EMA), carcinoembryonic antigen (CEA), wilm's tumor-1 (WT-1), CD34 and CD30 (*Figure 1*). Paratracheal lymph nodes were positive for metastasis, and the patient was given a diagnosis of MFH.

To explore the underlying molecular mechanisms and their potential therapeutic relevance, we utilized targeted next-generation sequencing (NGS) to detect driver mutations in tumor DNA (tDNA) with matched white blood cell (WBC) DNA as a control (sequencing depth

>1,000×; Beijing USCI Medical Laboratory Co., Ltd., China). A panel of 549 tumor-related genes was subjected to NGS (Supplementary method, *Figure S1*). The sequencing results identified five genes that each contained a single missense mutation (*Figure 2*). No copy number variation or gene translocation events were detected. Among the identified mutated genes, *TSC2* was detected at the highest frequency (15.64%).

Discussion

Since the first introduction in 1979, and the origin of MFH was always an enigma. Until 2012 MFH was declassified as a formal diagnostic entity and renamed as an undifferentiated pleomorphic sarcoma by the World Health Organization (WHO). This new terminology has been supported by a compelling body of evidence over the last decade to suggest that MFH is an aggressive soft tissue sarcoma originating from mesenchymal cells (1). MFH most frequently occurs in the extremities or retroperitoneal abdominal cavity (2), whereas pulmonary MFH is uncommon, accounting for less than 0.2% of pulmonary tumors (3).

We provide a literature review of primary pulmonary MFH patients as summarized in *Table 1*. Since 1990 there have been 20 published case reports of 23 primary pulmonary MFH patients (4-23). We have retrieved this literature and summarized the clinical features of these cases together with the case reported in the current study (*Table 1*). Coughing, hemoptysis and dyspnea were the most common symptoms, whereas shortness of breath, chest pain and weight loss were less frequently reported. In addition, 3 patients (13.04%) were asymptomatic such that MFH was discovered by CT scan during the course of a regular examination. There were more male MFH patients than female patients (14 vs. 9), and patient age ranged from 9 to 86 years old with a mean age of 52.87; 73.91% of these patients were between 40 and 80 years old at the time of diagnosis. Of these 23 patients, 3 were smokers, 5 were nonsmokers, and the remaining 15 had no specific record of smoking history. Thus, there is no obvious correlation of cigarette smoking with pulmonary MFH morbidity. There was no significant difference between the left and right lungs for MFH morbidity (30 vs. 31).

The documented information regarding tumor size is variable. One MFH patient with a tumor diameter of 1.7 cm lived for 108 months and still had no disease symptoms (3), while another patient with a tumor diameter of 11 cm died six months after diagnosis (19). This comparison suggests

that MFH patients with smaller tumors have a relatively good prognosis, although the overall prognosis for the disease is poor.

In general, the overall survival of reported cases ranged from 0 to more than 168 months. For these 23 patients, 5 patients did not receive any treatment and 2 patients received only chemotherapy or radiotherapy. In total, 15 patients underwent surgical resection, including 11 lobectomies, 3 pneumonectomies and 1 tumorectomy. In these 15 surgeries, 6 combined resection with neoadjuvant or adjuvant chemotherapy. Of these, 4 patients survived less than 12 months, 2 patients survived more than 12 months. Complete resection of tumors with systematic lymph node dissection is thought to contribute to the survival of patients with primary pulmonary MFH (4).

The diagnosis of primary pulmonary MFH is typically a multi-step process. First, a complete extrathoracic evaluation is made to confirm that MFH originated in the lung. Imaging techniques such as PET-CT are also utilized to arrive at a diagnosis of pulmonary MFH, which must be ultimately confirmed by histological examination. Histological sections can be obtained from preoperative puncture, tracheoscopic biopsy or postoperative tumor tissue. Maeda *et al.* (4) report that histological analysis for preoperative diagnosis is rare and only 4% of reported cases were histologically diagnosed before surgery. There are no specific immunohistochemical markers for MFH, however, other sarcomas with similar microscopic findings have been excluded with immunohistochemical staining. Desmin, actin, vimentin, keratin, and neurogenic tumors are commonly stained for the differential diagnosis. In the current case, no abnormalities other than the pulmonary mass were found by brain MRI, enhanced CT of abdomen and bone ECT examinations. The patient was then subjected to surgical resection, and subsequent immunohistochemical staining confirmed the diagnosis of MFH.

Molecular mechanisms responsible for primary pulmonary MFH formation and progression are mainly unknown. To explore possible underlying mechanisms, we performed NGS on postoperative tumor tissue. The resulting profiling data revealed five mutations in the *TSC2*, *ARID1B*, *CDK8*, *KDM5C* and *CASP8* genes. The mutation distribution diagrams of these genes from TCGA and highlighted in *Figure 2*. Among these, the mutation frequency of *TSC2* was 15.64%, which encodes a M280V missense mutation. The *TSC2* gene encodes tuberin, which is known to form heterodimers with hamartin (24). The tuberin/hamartin

Gene	Amino acid change	Frequency(%)
<i>TSC2</i>	M280V missense mutation	15.64
<i>ARID1B</i>	A329G missense mutation	3.28
<i>CDK8</i>	A68E missense mutation	2.17
<i>KDM5C</i>	R614Q missense mutation	1.94
<i>CASP8</i>	D217E missense mutation	1.68

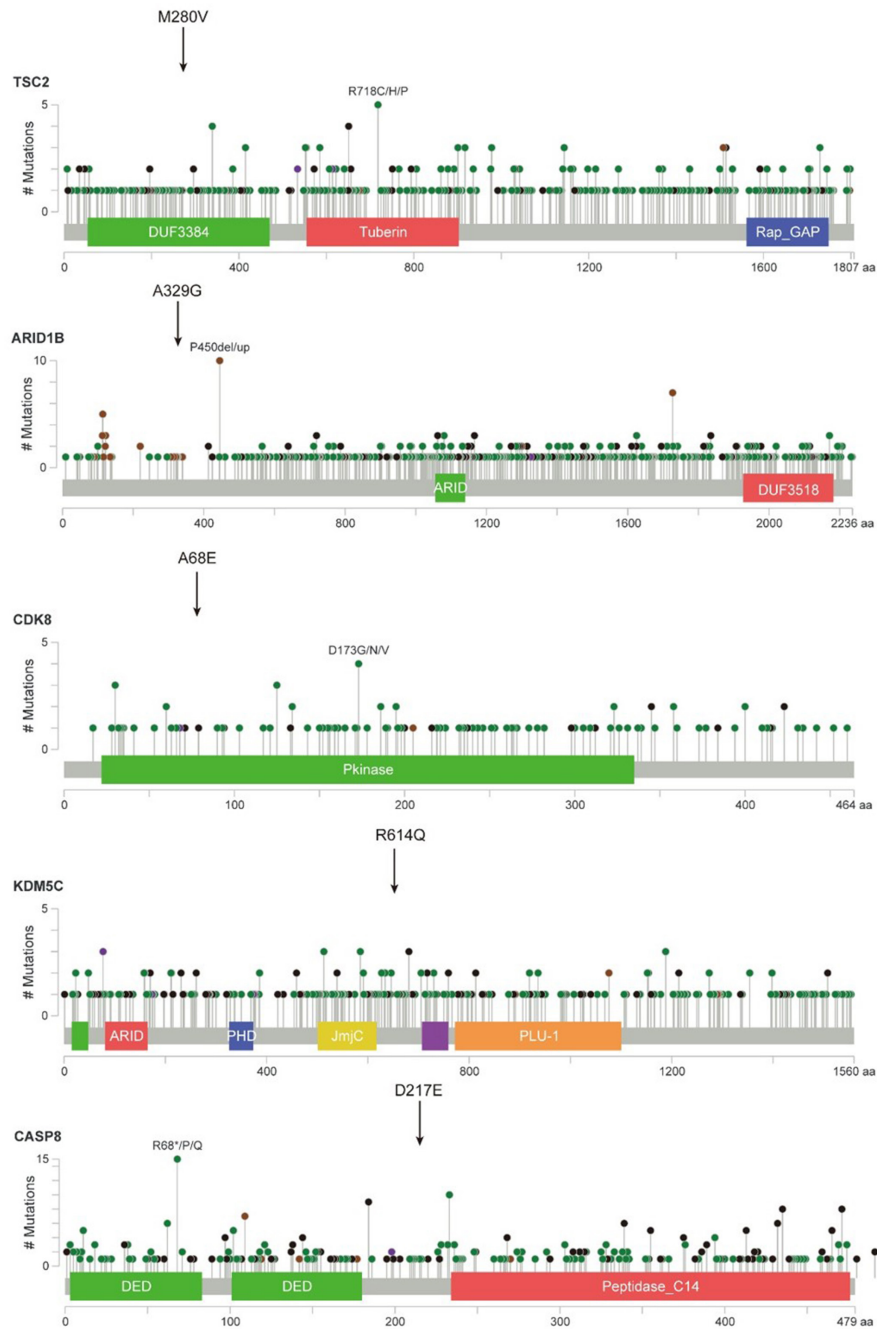


Figure 2 Gene mutation analysis results and corresponding data from The Cancer Genome Atlas (TCGA). The identified missense mutations in *TSC2*, *ARID1B*, *CDK8*, *KDM5C* and *CASP8* are overlaid with the mutation distribution diagrams of these genes from TCGA and highlighted with black arrows.

Table 1 Literature review of primary pulmonary MFH

Case	Reference	Age (years)	Sex	Smoke status	Site	Size (cm)	Symptoms at the admission	Treatment	LN	F/U	Survival (m)
1	Patel <i>et al.</i> (5)	86	M	NA	RLL	9.6×8.9×7.6	Cough, dyspnea, and increasing weakness	Lobectomy	NEG	NED	6
2	Li <i>et al.</i> (7)	80	F	NA	RUL	8	Cough	None	NA	DOD	1.5
3	Jeon <i>et al.</i> (8)	55	M	NA	LLL	NA	Cough and chest pain	Pneumonectomy/chemotherapy/XRT	NEG	NED	9
4	Thomas <i>et al.</i> (6)	47	M	No	RUL	NA	Swelling on the gingiva	Chemotherapy/XRT	POS	DOD	2
5	Tsangaridou <i>et al.</i> (9)	54	M	Yes	LUL/LLL	NA	NA	Pneumonectomy	POS	AWD	168
6	Maitani <i>et al.</i> (10)	18	F	NA	LUL	2.2	Asymptomatic	Partial lobectomy	NA	NED	36
7	Maeda <i>et al.</i> (4)	62	M	Yes	LUL	4.5×4	Asymptomatic	Lobectomy	POS	DNED	24
8	Noh <i>et al.</i> (11)	58	F	No	RUL	5×4	NA	Lobectomy/XRT	NEG	NED	5
9	Wang <i>et al.</i> (12)	86	M	No	LLL	9×15	Exertional dyspnea and poor appetite	None	NA	DOD	2
10	Alhadab <i>et al.</i> (13)	56	M	NA	LUL/LLL	NA	Cough and shortness of breath	None	NA	DOD	4
11	Herrmann <i>et al.</i> (14)	57	M	No	RUL	13×8	Car accident	Lobectomy	NA	NED	12
12	Fujita <i>et al.</i> (15)	65	F	NA	LL	12×12	Cough, yellow sputum and exertional dyspnea	None	NA	DOD	6
13	Barbas <i>et al.</i> (17)	37	M	Yes	RML/RLL	10×6×3	Cough, hemoptysis and weight loss	Pneumonectomy	NEG	DNED	6
14	Shah <i>et al.</i> (18)	9	M	NA	LUL	6	Cough, hemoptysis and weight loss	Lobectomy/XRT/chemotherapy	NA	NED	36
15	Nistal <i>et al.</i> (16)	12	F	No	LUL	7×6×5	Chest pain, fatigue, non-productive cough and weight loss	Lobectomy/chemotherapy	NA	AWD	5
16	Gómez-Román <i>et al.</i> (20)	61	M	NA	RUL	3	NA	Tumorectomy	NA	NED	9

Table 1 (continued)

Table 1 (continued)

Case	Reference	Age (years)	Sex	Smoke status	Site	Size (cm)	Symptoms at the admission	Treatment	LN	F/U	Survival (m)
17	Halyard <i>et al.</i> (19)	51	F	NA	LLL	10×8	Pleuritic chest pain	Lobectomy/XRT	NEG	NED	60
18		77	M	NA	RML	2.2	Asymptomatic	lobectomy	NEG	NED	36
19		40	M	NA	LLL	11×9×8	Cough, pain in the left posterior rib cage, weight loss, fatigue	Lobectomy/XRT/ chemotherapy	POS	DOD	6
20		57	F	NA	LUL	7.5×6×4	Ataxia, headache, and left homonymous hemianopsia	Lobectomy	NA	DOD	1
21	Kamath <i>et al.</i> (21)	56	M	NA	RLL	10	Blurred vision in the right eye	None	NA	DOD	3
22	Higashiyama <i>et al.</i> (22)	49	F	NA	RLL	6	Dry cough	Pneumonectomy	POS	NED	NA
23	In <i>et al.</i> (23)	43	F	NA	RLL	NA	Chest pain	Chemotherapy/ XRT	NA	NA	NA

MFH, malignant fibrous histiocytoma; LUL, left upper lobe; LLL, left lower lobe; RUL, right upper lobe; RML, right middle lobe; RLL, right lower lobe; NA, not available; XRT, radiotherapy; F/U, follow up; DOD, dead of MFH disease; AWD, alive with MFH disease; NED, no evidence of MFH disease; DNED, dead no evidence of MFH disease; m, month.

heterodimer inhibits the Rheb GTPase, leading to inactivation of the Rheb/mTOR/p70S6K pathway, which is a major regulator of cell growth and proliferation (24). Thus, deleterious mutations in TSC2 result in activation of the mTOR pathway, abnormal cell growth and increased proliferation. In non-small cell lung cancer, a previous study reported that targeting TSC2 can inhibit cancer cell growth (25). Therefore, we postulate that the TSC2 mutation identified here might be functionally involved in primary pulmonary MFH occurrence or progression, and mTOR inhibitors, such as everolimus, might be efficacious for some MFH patients.

In conclusion, based on the published literature reviewed here, MFH is insensitive to both chemotherapy and radiotherapy. Thus, once the diagnosis is confirmed, complete surgical resection is necessary. Targeted therapy using mTOR inhibitors might be a promising future treatment for this rare disease.

Acknowledgements

Funding: This work was supported by grants from the National Natural Science Foundation of China (81301812,

81172233), Specialized Research Fund for the Doctoral Program of Higher Education (20131202120004), Science & Technology Foundation for Selected overseas Chinese scholar Ministry of personnel of China, Science & Technology Foundation for Selected overseas Chinese scholar Bureau of personnel of China Tianjin, Tianjin Key Project of Natural Science Foundation (17JCZDJC36200), Tianjin Educational Committee Foundation (20120117) and Tianjin Medical University General Hospital Young Incubation Foundation (ZYYFY2015015).

Footnote

Conflicts of Interest: The authors have no conflicts of interest to declare.

Informed Consent: Written informed consent was obtained from the patient for publication of this manuscript and any accompanying images.

References

- O'Brien JE, Stout AP. Malignant fibrous xanthomas.

- Cancer 1964;17:1445-55.
2. Weiss SW, Enzinger FM. Malignant fibrous histiocytoma: an analysis of 200 cases. *Cancer* 1978;41:2250-66.
 3. Yousem SA, Hochholzer L. Malignant fibrous histiocytoma of the lung. *Cancer* 1987;60:2532-41.
 4. Maeda J, Ohta M, Inoue M, et al. Surgical intervention for malignant fibrous histiocytoma of the lung: report of a case. *Surg Today* 2007;37:316-9.
 5. Patel DP, Gandhi YS, Sommers KE, et al. Primary pulmonary malignant fibrous histiocytoma. *Case Rep Pulmonol* 2015;2015:381276.
 6. Thomas ME, Koshi R. Electron microscopy in the diagnosis of malignant fibrous histiocytoma of the lung presenting as metastasis to the maxillary gingiva. *Int J Oral Maxillofac Surg* 2013;42:99-101.
 7. Li JQ, Zhang JR, Li L, et al. Inflammatory malignant fibrous histiocytoma of the lung combined with fungal infection. *Chin Med J (Engl)* 2013;126:4379.
 8. Jeon YH, Park KS. Successful management of a recurrent primary malignant fibrous histiocytoma of the lung: report of a case. *Korean J Thorac Cardiovasc Surg* 2012;45:345-7.
 9. Tsangaridou I, Papamihalis G, Stathopoulos K, et al. Primary malignant fibrous histiocytoma of the lung: a case report. *Case Rep Med* 2010;2010:389692.
 10. Maitani F, Fujimori S, Hayashi Y, et al. A case of juvenile primary pulmonary malignant fibrous histiocytoma. *Tokai J Exp Clin Med* 2010;35:130-2.
 11. Noh HW, Park KJ, Sun JS, et al. Primary pulmonary malignant fibrous histiocytoma mimics pulmonary artery aneurysm with partial thrombosis: various radiologic evaluations. *Eur Radiol* 2008;18:1653-7.
 12. Wang CS, Tsai KB, Tsai JR, et al. Primary malignant fibrous histiocytoma of the lung: a case report. *Kaohsiung J Med Sci* 2003;19:428-32.
 13. Alhadab T, Alvarez F, Phillips NJ, et al. Malignant fibrous histiocytoma of the lung presenting as bronchial obstruction in a heart transplant recipient. *J Heart Lung Transplant* 2002;21:1140-3.
 14. Herrmann BL, Saller B, Kiess W, et al. Primary malignant fibrous histiocytoma of the lung: IGF-II producing tumor induces fasting hypoglycemia. *Exp Clin Endocrinol Diabetes* 2000;108:515-8.
 15. Fujita Y, Shimizu T, Yamazaki K, et al. Bronchial brushing cytology features of primary malignant fibrous histiocytoma of the lung. A case report. *Acta Cytol* 2000;44:227-31.
 16. Nistal M, Jimenez-Heffernan JA, Hardisson D, et al. Malignant fibrous histiocytoma of the lung in a child. An unusual neoplasm that can mimick inflammatory pseudotumour. *Eur J Pediatr* 1997;156:107-9.
 17. Barbas CS, Capelozzi VL, Takagaki TY, et al. Primary malignant fibrous histiocytoma of the lung. Report of a case with bronchial brushing cytologic features. *Acta Cytol* 1997;41:919-23.
 18. Shah SJ, Craver RD, Yu LC. Primary malignant fibrous histiocytoma of the lung in a child: a case report and review of literature. *Pediatr Hematol Oncol* 1996;13:531-8.
 19. Halyard MY, Camoriano JK, Culligan JA, et al. Malignant fibrous histiocytoma of the lung. Report of four cases and review of the literature. *Cancer* 1996;78:2492-7.
 20. Gómez-Román JJ, Val-Bernal JF. A case of malignant fibrous histiocytoma of the lung arising as a third primary tumor. *Thorac Cardiovasc Surg* 1996;44:321-3.
 21. Kamath SV, Tenreiro-Picon OR, Ragland RL, et al. Brain metastases from primary lung malignant fibrous histiocytoma: a case report. *J Neuroimaging* 1995;5:133-4.
 22. Higashiyama M, Doi O, Kodama K, et al. Successful surgery of malignant fibrous histiocytoma in the lung with gross extension into the right main pulmonary artery. *Thorac Cardiovasc Surg* 1993;41:73-6.
 23. In KH, Byun HJ, Kang KH, et al. A case of pulmonary malignant fibrous histiocytoma associated with pulmonary artery obstruction. *Korean J Intern Med* 1990;5:79-82.
 24. Benvenuto G, Li S, Brown SJ, et al. The tuberous sclerosis-1 (TSC1) gene product hamartin suppresses cell growth and augments the expression of the TSC2 product tuberlin by inhibiting its ubiquitination. *Oncogene* 2000;19:6306-16.
 25. Kwiatkowski DJ. Tuberous sclerosis: from tubers to mTOR. *Ann Hum Genet* 2003;67:87-96.

Cite this article as: Li X, Liu R, Shi T, Dong S, Ren F, Yang F, Ren D, Fan H, Wei S, Chen G, Chen J, Xu S. Primary pulmonary malignant fibrous histiocytoma: case report and literature review. *J Thorac Dis* 2017;9(8):E702-E708. doi: 10.21037/jtd.2017.07.59

Supplementary method

Next-generation sequencing

The panel was used to sequence all exons of 549 tumor-related genes mutations simultaneously (Figure S1). The concentration of the DNA samples was measured with the Qubit dsDNA assay to make sure that genomic DNA was 100 ng. Adjust the volume to a total of 100 µL using 1× TE (low EDTA) and transfer to a Covaris microTUBE for fragmentation. Fragment the gDNA so that the average DNA fragment size is 180–220 bp, followed by hybridization with the capture probes baits, hybrid selection with magnetic beads, and PCR amplification. A bioanalyzer high-sensitivity DNA assay was then used to assess the quality and size range. Available indexed samples were then sequenced on a Nextseq (Illumina, San Diego, CA, USA) with pair-end reads. Raw data from the

NEXT SEQ 500 runs were processed with flexbar software (version 2.7.0, <https://sourceforge.net/projects/flexbar/>) to generate clean fastq data, trim adapter sequences, and filter and remove poor quality reads. Then clean fastq data were aligned to hg19 (GRCH37) assembly by using BWA-sampe (Burrows Wheeler Aligner software version 0.7.12-r1039, <https://sourceforge.net/projects/bio-bwa/files/>), and PCR (polymerase chain reaction) duplicates were removed by MarkDuplicates tool in Picard Tools (version 1.124, <http://broadinstitute.github.io/picard/>). All variants were annotated using ANNOVAR (version 20160201, <http://annovar.openbioinformatics.org/en/latest/>). Variation frequency (>0.5%) was used to eliminate erroneous base calling and generate final mutations, and a manual verification was performed using IGV (Integrative Genomics Viewer version 2.3.72, <http://software.broadinstitute.org/software/igv/>).

A								
ABCB1	ABCC4	ABL1	ACVR1B	AKT3	APC	ARFRP1	ARID2	ATIC
ABCC1	ABCC6	ABL2	AKT1	ALK	AR	ARID1A	ASXL1	ATM
ABCC2	ABCG2	AKT2	AMER1	ARAF	ARID1B	ATF7IP	ATP7A	ATR
AURKB	ATRX	AXIN1	AURKA	AXL				
B								
B2M	BARD1	BCL2L2	BCORL1	BLK	BRAF	BRD4	BSG	BAP1
BAIAP3	BCL2	BCL6	BCR	BLM	BRCA1	BRIP1	BTG1	BCL2L1
BCOR	BIRC5	BMPR1A	BRCA2	BTK				
C								
C11orf30	CAMKK2	CBFB	CBR3	CCND3	CD19	CD33	CD52	CD79B
C18orf56	CARD11	CBL	CCND1	CCNE1	CD22	CD38	CD74	CDA
CAMK2G	CASP8	CBR1	CCND2	CCR4	CD274	CD3EAP	CD79A	CDC73
CDH1	CDK2	CDK6	CDK9	CDKN2A	CEBPA	CHEK1	CIC	CREBBP
CDK1	CDK4	CDK7	CDKN1A	CDKN2B	CHD2	CHEK2	CK1	CRKL
CDK12	CDK5	CDK8	CDKN1B	CDKN2C	CHD4	CHST3	COMT	CRLF2
CSF1R	CTCF	CTNNA1	CUL3	CYLD	CYP1A1	CYP1B1	CYP2B6	CYP2C8
CSK	CTLA4	CTNNB1	CYBA	CYP19A1	CYP1A2	CYP2A6	CYP2C19	CYP2C9
CYP2D6	CYP2E1	CYP3A4	CYP3A5	CYP4B1				
D								
DAXX	DDR1	DDR2	DNMT1	DNMT3A	DOT1L	DPYD	DSCAM	DAXX
E								
E2F1	EGFR	EML4	EPCAM	EPHA3	EPHA7	EPHB2	ERBB2	ERCC1
EGF	EGR1	ENOSF1	EPHA1	EPHA4	EPHA8	EPHB3	ERBB3	ERCC2
EGFL7	EMC8	EP300	EPHA2	EPHA5	EPHB1	EPHX1	ERBB4	ERG
ERRFI1	ESR1	ETV1	ETV4	ETV5	ETV6	EWSR1	EXT1	EXT2
EZH2								
F								
FAM46C	FANCE	FAS	FGF10	FGF3	FGFR2	FH	FLT3	FRK
FANCA	FANCF	FAT1	FGF14	FGF4	FGFR3	FKBP1A	FLT4	FRS2
FANCC	FANCG	FBXW7	FGF19	FGF6	FGFR4	FLCN	FOXL2	FUBP1
FANCD2	FANCL	FCGR3A	FGF23	FGFR1	FGR	FLT1	FOXP1	FYN
FZD7								
G								
GABRA6	GATA1	GATA3	GATA6	GID4	GLI1	GNA11	GNAQ	GPC3
GALNT14	GATA2	GATA4	GCK	GINS2	GLI3	GNA13	GNAS	GPR124
GRIN2A	GRM3	GSK3B	GSTM1	GSTM3	GSTP1	GSTT1		
H								
H3F3A	HCK	HGF	HIF1A	HIST1H3B	HNF1A	HRAS	HSD3B1	HSP90AA1
I								
IDH1	IGF-1	IGF2	IKBKB	IKZF1	INHBA	INSR/IR	IRF2	IRS2
IDH2	IGF1R	IGF2R	IKBKE	IL7R	INPP4B	IQGAP3	IRF4	ITIH5
ITK								
J								
JAK1	JAK2	JAK3	JUN					
K								
KAT6A	KDM5A	KDM5C	KDM6A	KDR	KEAP1	KEL	KIT	KLC3
KLHL6	KMT2A	KMT2B	KMT2C	KMT2D	KRAS			
L								
LCK	LIMK1	LMO1	LRP1B	LRP2	LYN	LZTR1	LCK	LIMK1
M								
MAGI2	MAP3K1	MAPK10	MAPKAPK2	MDM2	MEN1	MKNK2	MRC2	MSH6
MAP2K1	MAP4K4	MAPK14	MARK1	MDM4	MERTK	MLH1	MRE11A	MTDH
MAP2K2	MAP4K5	MAPK8	MAX	MED12	MET	MLH3	MS4A1	MTHFR
MAP2K4	MAPK1	Mapk9	MCL1	MEF2B	MITF	MPL	MSH2	MTOR
MTRR	MUTYH	MYC	MYCL1	MYCN	MYD88			
N								
NAT1	NBN	NCF4	NCOR1	NF1	NFE2L2	NKX2-1	NOTCH1	NOTCH3
NAT2	NCAM1	NCOA3	NEK11	NF2	NFKBIA	NOS3	NOTCH2	NPM1
NQO1	NRAS	NSD1	NTRK1	NTRK2	NTRK3	NUP93		
P								
PAK1	PARP2	PDGFRA	PIGF	PIK3R1	PLCG2	POLE	PRDX4	PRKCI
PAK3	PAX5	PDGFRB	PIK3C2B	PIK3R2	PLK1	PPARD	PRKAA1	PRKDC
PALB2	PBRM1	PDK1	PIK3CA	PPP1R13L	PMS1	PRRT2	PRKAR1A	PRSS8
PARK2	PDCD1	PHF6	PIK3CB	PKCγ	PMS2	PPP2R1A	PRKCA	PTCH1
PARP1	PDCD1LG2	PHKA2	PIK3CG	PRKCE	POLD1	PRDM1	PRKCB	PTEN
PTK2	PTPN11	PTPRD	PTK6					
Q								
QKI								
R								
RAC1	RAD50	RAD51C	RAF1	RARA	RBM10	RHPN2	RMDN2	ROCK1
RAC2	RAD51	RAD51D	RANBP2	RB1	RET	RICTOR	RNF43	MST1R
ROS1	RPL13	RPS6KA1	RPS6KB1	RPTOR	RRM1	RUNX1	RUNX1T1	
S								
KITLG	SDHD	SKP2	SLC22A6	SMAD4	SOD2	SPOP	STAT1	STAT6
SDHA	SETD2	SLC10A2	SLCO1B1	SMARCA4	SOX10	SPTA1	STAT2	STEAP1
SDHAF1	SF3B1	SLC15A2	SLCO1B3	SMARCB1	SOX2	SRC	STAT3	STK11
SDHAF2	SGK1	SLC22A1	SLIT2	SMO	SOX9	SRD5A2	STAT4	STK3
SDHB	SHH	SLC22A16	SMAD2	SNCAIP	SPEN	SRMS	STAT5A	STK4
SDHC	SIK1	SLC22A2	SMAD3	SOCS1	SPG7	STAG2	STAT5B	SUFU
SULT1A1	SULT1A2	SULT1C4	SYK					
T								
TAF1	TCF7L2	TNF	TNFRSF8	TET2	TK1	TOP1	TPMT	TSC1
TBX3	TEK	TNFAIP3	TNFSF11	TGFBR1	TMEM127	TOP2A	TPX2	TSC2
TCF7L1	TERT	TNFRSF14	TNFSF13B	TGFBR2	TMPRSS2	TP53	TYRO3	TYMS
TSHR	TNK2	TNFRSF10B	TNFRSF10A					
U								
U2AF1	UBE2I	UGT1A1	UGT2B15	UGT2B17	UGT2B7	UMPS	U2AF1	UBE2I
V								
VEGFA	VEGFB	VHL						
W								
WEE1	WISP3	WNK3	WT1					
X								
XPC	XPO1	XRCC1	XRCC4					
Y								
YES1								
Z								
ZAP70	ZBTB2	ZC3HAV1	ZNF217	ZNF703				

Figure S1 Next-generation sequencing to identify mutations in 549 tumor-related genes.